General Disclaimer

One or more of the Following Statements may affect this Document

- This document has been reproduced from the best copy furnished by the organizational source. It is being released in the interest of making available as much information as possible.

- This document may contain data, which exceeds the sheet parameters. It was furnished in this condition by the organizational source and is the best copy available.

- This document may contain tone-on-tone or color graphs, charts and/or pictures, which have been reproduced in black and white.

- This document is paginated as submitted by the original source.

- Portions of this document are not fully legible due to the historical nature of some of the material. However, it is the best reproduction available from the original submission.

NATIONAL AERONAUTICS AND SPACE ADMINISTRATION

Technical Memorandum 33-728

Final Report on the Detection of Geothermal Areas from Skylab Thermal Data

Barry S. Siegal
National Research Council
Resident Research Associate
at
Jet Propulsion Laboratory

Anne B. Kahle
Alexander F. H. Goetz
Alan R. Gillespie
Michael J. Abrams
Jet Propulsion Laboratory

Howard A. Pohn
U.S. Geological Survey

JET PROPULSION LABORATORY
CALIFORNIA INSTITUTE OF TECHNOLOGY
PASADENA, CALIFORNIA

June 15, 1975

PREFACE

The work described in this report was performed by the Space Sciences Division of the Jet Propulsion Laboratory.

CONTENTS

ABSTRACT

Skylab-4 X-5 thermal data of The Geysers area was analyzed to determine the feasibility of using midday Skylab images to detect geothermal areas. The hottest ground areas indicated on the Skylab image corresponded to south-facing barren or sparsely vegetated slopes. Thermal well #4, a geothermal area approximately 15 by 30 m coincided with one of the hottest areas indicated by Skylab. However, this area could not be unambiguously distinguished from the other areas which are believed to be hotter than their surroundings as a result of their topography, and micrometeorological conditions. A simple modification of Watson's thermal model was performed and the predicted temperatures for the hottest slopes using representative values was in general agreement with the observed data. It is concluded that data from a single midday Skylab pass cannot be used to locate geothermal areas.

INTRODUCTION

Geothermal exploration has received considerable attention within the past several years as a result of the increased demand for energy. Areas favorable for such exploration have, in general, been recognized from field reconnaissance and by remote sensing from aircraft. Although remote sensing techniques have been utilized for almost a decade, until the advent of Skylab, no non-military satellite had sufficiently high thermal or spatial resolution to detect these areas.

Theoretically, the ideal times for detection of such areas are postdawn and at sunset (Watson, 1975). The effects of thermal inertia of surface materials are minimized at these times. Unfortunately, Skylab data acquisition times do not coincide with these optimal times. The present study was undertaken to determine if data from a Skylab near-noon pass could be used to detect a known geothermal area.

The study area chosen was the Geysers geothermal field in Sonoma County, California, which is one of the few producing geothermal fields in the world. This area has been studied extensively using both ground and aerial survey techniques, (see Allen and Day, 1927; Cal. Div. Mines and Geol., 1966; McNitt, 1968; Moxham, 1969; Stanley, et al., 1973; U.S.G.S., 1973; Chapman, 1975), and more recently by the Martin-Marietta Company (1974) using Skylab nighttime data.

Data analyzed was acquired by one experiment carried out in the Skylab missions, the S 192 multispectral scanner. This scanner imaged the ground in 13 wavelength bands in the visible, reflective infrared and thermal infrared. Data was recorded in a 68.5 km swath about the spacecraft ground track.

Two different detectors were used for the thermal infrared channel (10.2 to 12.5 μm) at various times during the 3 missions. The Y-3 detector was used for the first two missions, and part of the third. It had a theoretical thermal

resolution of 0.7°C, but due to excessive noise, this resolution was not realized, and the detector was replaced by the X-5 detector during the third mission. The actual NEΔT of this detector was approximately 0.67°C. Only data from the X-5 detector was used in this study.

DESCRIPTION OF THE SITE

Geography and Topography

The Geysers geothermal area is located in Sonoma County, California, 100 km north-northwest of the city of San Francisco. An area approximately 15 by 12 km was chosen for study (Figure 1).

The topography of this region is characterized by northwest trending valleys and ridges. Relief varies from 400 to 1100 meters (Figure 1). Drainage for the area is through Big Sulfur Creek, Squaw Creek, and Little Sulfur Creek, which all feed into the Russian River to the southwest. The climate is Mediterranean, and most of the precipitation occurs in the winter; summers are hot and dry. Vegetation consists of seasonal grasses, scrub bushes and some trees.

The main geothermal activity occurs in the valley occupied by Big Sulfur Creek and along Geyser Canyon, trending north from The Geysers Resort. The south-facing slopes along Big Sulfur Creek are barren or sparsely grass covered with occasional scrub brush and trees along drainages, whereas north-facing slopes are predominantly tree covered.

Geology

The Geysers area is underlain by the Jurassic-Cretaceous Franciscan Assemblage, a complex eugeosynclinal sequence of chert, greenstone, graywacke and sedimentary breccia, and sedimentary and tectonic melange. The Franciscan Assemblage is overlain by Jurassic (?) metamorphosed ultramafic rocks and serpentine.

Extrusive volcanic rocks of Pliocene-Pleistocene age occur near the study area. These include the Clear Lake series, which extends to within 8 km of The Geysers area, and rhyolite flows which cap Cobb Mountain just northeast of the area.

The area has undergone complex faulting, trending predominantly northwest, producing a series of horsts and graben. The individual horsts and graben are 2-3 km wide and extend for up to 15 km (Figure 2).

The Geysers is one of numerous thermal areas within one of these northwest-trending graben. McNitt's (1968) interpretation indicates 4 km of vertical displacement along this graben. It is possible that this displacement has provided channels for the ascension of heated fluids, which could be the source for geothermal activity in the area.

Recent detailed geologic mapping of The Geysers region by McLaughlin (1974) shows that the area is extensively covered by Quaternary landslide deposits. Hydrothermal alteration is prevalent, predominantly along fault zones, and transcends lithologic boundaries.

Geothermal Development of Region

Geothermal activity was first discovered in The Geysers area in 1847, and the region soon became a well-known health resort. The first wells were drilled in 1921 for the purpose of generating electric power. By 1925, eight wells were completed; however, because of the lack of a market for steam-generated electricity, the project was discontinued.

Development resumed in 1958 when the Pacific Gas and Electric Company contracted with Magma Power Company and its partner Thermal Power Company to build a steam-electric power plant. This plant (units 1 and 2 in Figure 3) went into final production in 1963, and now generates 24,000 kilowatts of electricity by steam.

To date, a total of six power plant units have been built, five are operational. Each unit consists of a generating plant approximately 20 by 40 meters, and a cooling unit, approximately 40 by 100 meters. Steam is supplied to these

plants from numerous nearby wells (Figure 4). Total power production in 1974 was approximately 400,000 kilowatt of electricity, enough to supply the needs of a city half the size of San Francisco.

DIGITAL DATA PROCESSING

Skylab digital data of The Geysers geothermal area was obtained from Johnson Space Center on computer compatible magnetic tapes. Reflected and emitted radiation was recorded by the S-192 multispectral scanner in thirteen discrete wavelength bands, of which six were used (Table 1). The instantaneous field of view of one picture element (pixel) is approximately 75 by 75 meters. These data were processed by the Image Processing Laboratory at JPL.

TABLE 1.   Wavelength of Selected Skylab S-192 Channels

SDO #	Wavelength (µm)
03	.56 - .61
07	.68 - .78
09	.78 - .88
11	1.55 - 1.75
15	10.20 - 12.50
19	.98 - 1.03
21	10.20 - 12.50

A geometric correction was applied to the digital data, unmodified in the delineated study area, to compensate for skew caused by the earth's rotation during acquisition of the image. The image was then resampled digitally to improve the registration to established topographic base maps of The Geysers region. Contrast in the rectified image was then increased to distribute measured brightness levels (DN) over the entire dynamic range of the photographic film used for display of the digital image. This process increases the investigator's ability to discern contrast variations in the picture. Prior to contrast enhancement a probability

density function (PDF) was created which describes the frequency of occurrence of DN within an image. An appropriate contrast stretch was derived based upon the PDF. The PDF was also used to identify the brightest 100 and 300 pixels, corresponding, in the thermal image, to the hottest points (Figures 5 and 6).

Ratioing of two reflective channels was used to reduce the effect of topography on radiometry, thus enhancing spectral information. Ratioing consists of dividing, pixel by pixel, the DN values of the images, and encoding these ratios as DN to form a new image.

A detailed description of these techniques is given by Billingsley and Goetz (1973).

DATA ANALYSIS

Preliminary Analysis

As a first step in the recognition of the hottest ground areas within The Geysers region, a probability density function (as described above) of ground temperatures was produced from the Skylab-4 X-5 near-noon pass. No anomalous hot spots were detected from an analysis of the thermal channel data (SDO-21). Rather, ground temperatures were normally distributed. If geothermal areas are to be distinguishable, their temperature must be significantly higher than their surroundings. Therefore, computer enhancement techniques, as discussed previously, were used to delineate the hottest 100 and 300 ground areas (pixels). These results are displayed in Figures 5 and 6. The hottest areas are black, decreasing ground temperatures are in diminishing shades of gray, and the coolest areas are white. Although there appears to be an extreme contrast between the hot areas and their surroundings, this is due to the enhancement procedure; actual temperatures differ less than 1°C between the black and the darkest gray regions. Stream channels and other pronounced physiographic features can be recognized and matched to the same features in the topographic map (Figure 1).

From inspection of Figures 5 and 6, it is apparent that all of the hottest areas occur on south-facing slopes. It is also apparent that the clusters of the top 300 pixels are primarily an expansion of the clusters of the top 100, indicating that these are probably true hot areas and not noise in the data. Inspection of aerial photographs indicates that almost all of these areas occur on bare ground. These observations would be expected as a result of normal midday solar heating.

Comparison of the top 100 and 300 pixels with the most recent detailed geologic map of The Geysers region (Figure 2) indicates that the hottest areas appear to be independent of lithology. Comparison of these areas with published data on the location of known geothermal areas and related man-made structures (Figures 3 and 4) shows only slight coincidence.

The obvious relationship between topography and solar heating introduces the strong possibility that all the hot areas were those most favorably oriented to receive solar radiation. Therefore scatter diagrams of the temperature of the top 300 pixels (expressed in DN) vs. angle of incidence of solar radiation on these slopes were produced. The scatter of points was too large to determine a relationship between these variables. Separate scatter diagrams were produced for the major geologic units in order to determine if this scatter was due to the variability in surface properties of different lithologies. No relationship could be established. Despite these negative results, a relationship should exist between ground temperature and angle of incidence of solar radiation. The most probable cause for this scatter was that an insufficient range of temperature data was being analyzed. Therefore, a more thorough quantitative analysis, with a larger data base, was undertaken.

Quantitative Analysis

As a first step in the quantitative analysis, an attempt was made to superimpose precisely the Skylab image on topographic maps (The Geysers and Asti,

California 7 1/2' quadrangles) containing the study area. Due to the lack of resolution of prominent topographic features within the Skylab data and minor distortions, individual pixels could not be located exactly. Because of this uncertainty, a 3 x 3 pixel average was used to reduce this source of error. The 3 x 3 pixel grid was placed on the topographic maps and the slope angle and azimuth were measured in two selected regions for 924 9-pixel groups. These two regions contained the majority of the highest temperatures and the known geothermal areas.

To minimize the effects of vegetation, only the 145 9-pixel groups were analyzed which coincided with barren or sparsely grass covered areas as identified on aerial photographs. The cosine of the angle between the normal to these slopes and incident solar radiation was plotted against the average DN value (Figure 7). The expected relationship between temperature and solar radiation is apparent, in contrast to the previous analysis of only the top 300 pixels. If areas with significant geothermal heating are present, their distribution of points on Figure 7 should lie above and to the left of the main distribution. The large scatter of data precludes unambiguous identification of any geothermally heated area in the study region. Furthermore, refinement by analyzing each geologic unit separately did not reduce the scatter.

A contingency table was constructed and a chi square test was performed to determine the association between the bare areas and the clusters of the pixels representing the 100 hottest temperatures which were contained in the two selected regions (see Table 2). The observed association between bare areas and hot spots is indicated in Table 2a. If these variables are independent, the expected relationship would be that given in Table 2b. A chi square test was performed on the tabulated values to determine the significance of the observed relationship. Chi square is calculated from

$$\chi^2 = \sum_{i=1}^{4} \frac{(O-E)^2}{E},$$

where

    0 = Observed

    E = Expected.

For the observed association χ^2 = 102.6. According to statistical tables,
(Arkin and Colton, 1963), the expected χ^2 value for 1 degree of freedom at
P_{001} is 10.8. This implies that the observed association between bare areas
and hot spots would occur by chance much less than once in a thousand.

Table 2. Contingency Table

(a) Observed

	Ground Cover		
	Bare	Not Bare	Total
Hot	24.	7.	31.
Not Hot	169.	1143.	1312.
Total	193.	1150.	1343.

(b) Expected If Independent

	Ground Cover		
	Bare	Not Bare	Total
Hot	4.45	26.55	31.
Not Hot	188.55	1123.45	1312.
Total	193.	1150.	1343.

The association between bare areas and hot spots, and the importance of
the topographic control on solar heating required the introduction of computer
data handling techniques to evaluate and then remove the effects of these vari-
ables. Digital topographic data of The Geysers region were provided by Honeywell

Marine Systems Division, West Covina, California. These data were extracted from the 1:250,000 topographic map of the Santa Rosa quadrangle, and consisted of the ground elevation in feet on a 208.33 foot (63.5 meters) orthogonal grid. For this established grid, the slope angle and azimuth were computed from the digital data. The amount of solar radiation incident on these slopes was computed from an existing atmospheric model (Gates et al., 1971). The results are displayed in Figure 8. The intensity of incident radiation is displayed in various gray levels with white being the most intense. The Skylab data were converted to the topographic coordinate system to compare the thermal data with the solar irradiation data. It is apparent that the slope information derived from the digital topographic data lacks the resolution necessary to match accurately the detail provided from Skylab.

Because the effects of vegetation on surface heating have not been quantified techniques refined by Rowan et al. (1974) were used in an attempt to identify vegetated areas and remove them from the data set. Ratio pictures of the various Skylab spectral bands were produced for this purpose. Figure 9 is a ratio of SDO 3 (.56 to .61 μm) to SDO 7 (.68 to .76 μm) and is typical of the ratio pictures produced from the Skylab data. Unfortunately, this procedure also enhances the noise and it is apparent that in this data the noise obscures any new meaningful information.

Despite the lack of success in removing completely the effects of topography and vegetation, the analysis provided valuable insight into the magnitude of these effects.

DETECTABILITY OF GEOTHERMAL AREAS BY SATELLITE

Ground temperatures are determined by measuring the flux of ground infrared radiation which reaches the spacecraft sensors. The sensor integrates the flux over a resolution element and provides a signal corresponding to an area weighted average temperature after calibration. For the purposes of this investigation,

a simple calculation was performed to determine the size and temperature
of a surface geothermal feature which could be detectable by Skylab. The
effects of atmospheric absorption were ignored.

The flux emitted by a surface of temperature T is $\epsilon \sigma T^4$, where ϵ is the
emissivity of the surface, which is assumed here to be 1.0, and σ is the
Stefan-Boltzmann constant.

The Skylab thermal imaging system yields an average temperature over
a ground area, A, of approximately 75 meters by 75 meters. If a smaller
area, a, at a hotter temperature, T_H, exists within the resolution element
A, the measured value (T_s) will be the total flux from the various temper-
ature sources

$$A \sigma T_s^4 = a \sigma T_H^4 + (A - a) \sigma T_g^4$$

where T_g is the average temperature of the remainder of the pixel. Solving
for a we have

$$a = \frac{A(T_s^4 - T_g^4)}{(T_H^4 - T_g^4)}$$

This equation can be used to establish the size and temperature of an
anomalously hot area which could be detected by Skylab sensors. This
anomalously hot area must be hot enough and/or large enough to raise
the integrated temperature sensed by the satellite, T_s, significantly higher
than the temperature of the surrounding pixels. A background temperature,
T_g, of 280°K is assumed for the normal temperature of the sensed pixel and
its surroundings. The size and temperature relationship for detectability
at various levels of T_s above the background temperature, T_g, are shown in
Figure 10. For example, a hot area 16 meters by 16 meters at a temperature
of 360°K would raise the sensed temperature, T_s, by 5° to 285°K. Clearly,

geothermal areas must be hot and/or large to be unambiguously detected by Skylab sensors. Published reports and maps of The Geysers area indicate no naturally occurring hot springs or steam vents that fulfill the detectability requirements. There is, however, one large anomalously hot region, which is detectable: thermal well #4 (see discussion on Field Reconnaissance).

In contrast to the convective transport of hot fluids, which creates only isolated small hot spring and steam vents in The Geysers area, surface areas considerably larger than the areal extent of a pixel can be heated by conduction. Although the satellite will be able to detect these elevated temperatures as long as they are above the noise level of the sensors (approximately $1^{\circ}C$), these areas cannot be positively identified as geothermal regions without consideration of all the other components of the surface heat balance equation. These include solar heating, terrestrial radiation, atmospheric radiation, latent heat of evaporation, and sensible heat transport into the atmosphere. All of these are one to several orders of magnitude larger than the geothermal heat flux which will be induced by the known temperature gradients in The Geysers area. With a temperature gradient of $20^{\circ}C/100$ m and a conductivity of .01 cal/$^{\circ}K$ cm sec the geothermal heat flux would be 20 heat flow units (HFU). Hase (1971) in studies at Yellowstone National Park, Wyoming, has suggested that a geothermal heat flow must be greater than 240 HFU to be detectable by any method. Based on a theoretical model Watson (1975) has shown that with only a single temperature measurement the error in the heat flux can easily vary from 250 to 1000 HFU. Therefore, even though the possibility exists of enhancement of surface temperatures in The Geysers area due to geothermal heating by conduction, recognition of such areas is highly unlikely.

FIELD RECONNAISSANCE

Field reconnaissance was undertaken in The Geysers region to try to deter-
mine the nature of the heating processes occurring at the location of the
pixels representing the hottest temperatures. One cluster of these pixels
(cluster A in Figure 5) coincided with the highest thermal anomaly seen by
Moxham (1969) in daytime and nighttime infrared images of The Geysers region.
This area includes a large geothermal region of boiling surface waters and
steaming ground about a blown-out steam well, thermal well #4. The highest
temperature value within the cluster occurs at the well location.

The hottest ground temperatures within this region occur in a hydrothermally
altered area approximately 15 by 30 meters. Although measurements of subsur-
face temperatures at a depth of a few centimeters were consistently near boiling,
surface occurrences of boiling water and steam are patchy. Between these very
hot areas, surface temperatures were only slightly to moderately elevated due
to apparent evaporative cooling.

Several drilled vents in the immediate area are forcefully venting steam,
which combined with the steaming ground, produced a large steam cloud over
the entire area, to a height of about 100 meters. Temperature of the venting
steam at the smallest drilled hole was 125°C at the top of the well casing,
decreasing to 70°C two meters above the well casing.

Although steam wells, small steam vents and minor surface springs were
observed in the immediate surrounding areas corresponding to the remaining
pixels in cluster A, it was impossible to determine if there was sufficient
geothermal heat flow to enhance measurably the surface temperature. These
regions are steep, barren or sparsely grass covered, have south-facing slopes,
and receive substantial solar heating.

Based upon these field observations, it appears certain that the geo-thermal heati... about thermal well #4 was detected by Skylab. The actual temperature measured by Skylab was 25°C for the pixel coinciding with thermal well #4, which is 4°C hotter than its surroundings. This temperature is rea-sonable in view of the effects of evaporative cooling, masking of the ground by steam clouds, and averaging of temperatures over an area larger than the anomalously hot region about thermal well #4.

An extensive network of steam pipes leads from the wells to power plants and cooling units in many parts of the study area. None of these structures are hot enough or large enough to be identified by Skylab.

The hottest temperature within The Geysers region did not occur near thermal well #4 nor near any other known geothermal site. It is located above Squaw Creek (Cluster B in Figure 5) on a steep, barren, southeast-facing slope comprised of dark greenstone. Between outcrops, slopes were thinly covered with dry grass. No surface indications of geothermal activity were found.

Clusters C and D are located above Squaw Creek and also contained some of the hottest temperatures (Figure 5). They were similar in all respects to Cluster B.

Cluster E is located on the northwest side of Cobb Creek (Figure 5). The southeast-facing slopes are more heavily grass covered, less steep, and have fewer rock outcrops than the Squaw Creek locations. The slopes are concave and form a sheltered valley. Therefore, local meteorological effects may be significant in the heating of this region. Minor occurrences of warm springs indicate geothermal activity in the general vicinity, which may also enhance the heating.

Cluster F on Figure 5 is located at the abandoned Cloverdale Mine. Although it does not include one of the highest 10 temperatures, this cluster was investigated because of the mapped occurrence of hydrothermally altered rocks, (Figure 2) and reports of H_2S gas. The slopes are steep, southeast facing and sparsely grass covered. Extensive mine dumps of chert mantle the slopes below the Cloverdale Mine. The hottest temperature in the cluster coincided with graywacke outcrops above the dumps. No geothermal activity was noted.

All the aforementioned locations except thermal well #4 had concave, sheltered slopes, though to a lesser degree than at Cobb Creek.

Areas of known but unpublished geothermal activity were investigated and no correlation could be found with the top 300 pixels on the Skylab image. All of these areas were either heavily vegetated or located on flat, west-facing or north-facing slopes.

THERMAL MODELING

Thermal modeling was undertaken to explain the occurrence and distribution of the hottest ground areas within The Geysers region. This investigation stemmed from the observation that the hottest ground temperatures were, without exception, on south-facing slopes. In addition, the effects of topography on solar heating in an area of rugged terrain, such as The Geysers, should be expected to overwhelm the very subtle effects of geothermal heating of the surface.

The thermal model used in this study was developed by Watson (1971; Watson, et al., 1971; Watson, 1973, 1975). This model explains the surface temperature behavior of the ground through a diurnal cycle. Watson, (1975) indicated that a sampling frequency of three or four measurements during a

single diurnal cycle would be required to unambiguously identify geothermal anomalies below 100 heat flow units under ideal conditions. However, if data can be acquired only once during a diurnal cycle, the optimum time would be either at sunset or shortly after sunrise. Neither of these time constraints was met with the Skylab-4 overflight data of The Geysers region. Nevertheless, an attempt was made to explain the distribution of hot spots within The Geysers region by using representative values for the necessary parameters in Watson's model.

The temperature values and locations of the pixels were transferred to a topographic map of The Geysers and the local dips and azimuths were read for the 15 hottest slopes in the scene.*

An examination of the S-190 B photograph of The Geysers area showed that each of the slopes had a high albedo and was barren of any significant amount of vegetation. The values for the 15 slopes (dip, azimuth, and temperature averaged over the slope) were incorporated into the Watson model in an attempt to find a single set of values of thermal inertia and albedo which would most closely match the observed temperature of these slopes in the S-192 data. The parameters for the initial model were as follows: thermal inertia = .035 cal cm^{-2} sec$^{-\frac{1}{2}}$, albedo = .55, emissivity = .95, sky temperature = 260°K, cloud cover factor = .20. These parameters are consistent with a mixture of soil and rock with a high albedo. Thermal inertias of soils generally vary from .010 to .040 cal cm^{-2} sec$^{-\frac{1}{2}}$, rock from .040 - .090 cal cm^{-2} sec$^{-\frac{1}{2}}$.

---

*The selection of slopes was based on the presence of a cluster of several pixels whose individual temperatures were at least 18°C. The geographic limits of the pixels accepted for any given slope were determined by any significant change in dip or azimuth of the slope (in each case, between 9 and 15 pixels).

Although the temperature extremes for the 15 slopes were only 6.9°C for the Skylab data, the model predicted a temperature difference of 10.0°C. Any variation in the parameters which would reduce the predicted temperature difference necessitated the use of unrealistic values of cloud cover, sky temperature, or emissivity. A plot of azimuth versus midday temperature generated in the initial model for various dips is shown in Figure 11.

A modification of the Watson model was made which assumed that slopes across the valleys from the measured slopes occulted a significant fraction of the sky. Because north-facing slopes were nearly at sky temperature, only a small modification of sky temperature was necessary for south-facing slopes. However, the south-facing slopes were found to be 30 to 35°C hotter than the sky and a large adjustment in sky temperature was necessary for north-facing slopes. East-and west-facing slopes were intermediate in value.

A simplistic modification of the initial model was assumed: that each of the 15 slopes was looking at a 30 degree opposite-facing slope which occulted one-third of the sky, and sky temperatures were adjusted accordingly. No additional correction was made for reradiation and reflection between surfaces, although the effects were clearly important.

Figure 12 is a plot of temperature generated in the modified model versus azimuth for various dips. The lowest temperatures attained in this model are -2.5°C, a value which is compatible with the S-192 temperatures.

The data from this model was compared to temperatures from the Skylab thermal channel. Figure 13 is a plot of the angle between the sun and surface normal, versus temperature for the 15 hottest slopes. A 1.1°C correction factor was added for atmospheric attenuation. There is very close agreement between observed and predicted temperatures. Consequently, explanation of the hot areas does not require geothermal heating.

ANALYSIS OF NORTH-FACING SLOPES

The highest temperatures in The Geysers region coincide with bare, south-facing slopes. To reduce the effect of solar radiation, analysis of nighttime images is desirable. Data for the only nighttime pass of The Geysers region was examined, but because of the exceptionally high noise level, was not considered.

Therefore, an attempt was made to make use of shadowed steep-slope areas as simulated nighttime images. The temperatures of these north-facing slopes were extracted for the daytime X-5 thermal channel (SDO 21). The highest 100 temperatures within these regions were set to black and displayed in picture form (Figure 14). Within the accuracy of pixel location, the ground areas with highest temperatures coincided with marginally sunlit ridges or slopes. No correlation was found between these pixels and geothermal areas on the north-facing slopes.

SUMMARY AND CONCLUSIONS

Skylab X-5 thermal data for a daytime pass over The Geysers geothermal field was analyzed to determine the feasibility of using Skylab to detect geothermal areas. The hottest ground areas were identified on the Skylab image and were located on topographic maps, aerial photographs, and in the field.

In conclusion, the following statements can be made:

1) The hottest areas found on the S-192 thermal images in The Geysers region are all found on south-facing slopes which are barren or sparsely vegetated.

2) No statistically significant association exists between the hottest areas on Skylab thermal images and known geothermal areas in The Geysers region. This result is consistent with the temperature and spatial resolution capability of the S-192 scanner, and published field data of the area.

3) Although thermal well #4 coincides with a pixel which represents hot ground, it cannot be unambiguously distinguished from areas believed to be hotter than their surroundings as a result of their topography, micrometeorlogical conditions, and insolation.

4) A simple modification can be made in the Watson model which considers reradiation from opposite facing slopes. This modification produces a close agreement between observed and predicted temperatures without requiring geothermal heating.

ACKNOWLEDGMENTS

REFERENCES

Allan, E., and Day, A., 1927, Steam Wells and Other Thermal Activity at "The Geysers" California: Carnegie Inst. Washington pub. 378, 106 pp.

Arkin, H. and Colton, R., 1963, Tables for Statisticians: Barnes and Noble, Inc., New York, 168 pp.

Billingsley, F., and Goetz, A., 1973, Computer Techniques Used for some Enhancements of ERTS Images: Symposium on Significant Results Obtained from Earth Resources Technology Satellite-1, NASA SP-327, pp. 1159-1167.

California Division of Mines and Geology, 1966, Gravity Map of Geysers Area, Mineral Information Service, Vol. 19, 148-149.

California Division of Oil and Gas, 1974, The Geysers Geothermal, map G6-1.

Chapman, Rodger H., 1975, Geophysical Studies in the Clear Lake Region, Calif., Calif. Div. Mines and Geology, Special Rpt. #117, (in press).

Gates, W., Batten, E., Kahle, A., and Nelson, A., 1971, A Documentation of the Mintz-Arakawa Two-Level Atmospheric General Circulation Model: The Rand Corp., R-877-ARPA, 408 pp.

Hase, H., 1971, Surface Heat Flow Studies for Remote Sensing of Geothermal Resources: Proc. 7th Internatl. Symposium on Remote Sensing of Environment, Univ. Michigan, V. 1, pp. 237-246.

Martin-Marietta Corporation, 1974, EREP Geothermal Final Report: NASA Contract NAS8-24000, 65 pp.

McLaughlin, R., 1974, Preliminary Geologic Map of The Geysers Steam Field and Vicinity, Sonoma County, California: U.S.G.S. open file map.

McNitt, J., 1968, Exploration and Development of Geothermal Power in California: California Division of Mines and Geology Special 75, pp. 1-44.

Moxham, R., 1969, Aerial Infrared Surveys at The Geysers Geothermal Steam Field, California: U.S.G.S. Professional Paper 650-C, pp. C106-C122.

Rowan, L., Wetlaufer, P., Goetz, A., Billingsley, F., and Stewart, J., 1974 Discrimination of Hydrothermally Altered Areas and of Rock Types Using Computer Enhanced ERTS Images, South-Central Nevada: U.S.G.S. Prof. Paper, #883.

Stanley, W. D., Jackson, D. B., and Hearn, B. C., 1973, Preliminary Results of Geoelectrical Investigations Near Clear Lake, Calif., U.S.G.S. Open File Rpt. #73-270

U.S.G.S., 1973, Aeromagnetic Map of the Clear Lake Area, Lake, Sonoma, Napa and Mendocino County, Calif., Open File Rpt. #73-299.

Watson, K., 1971, A computer Program for Thermal Modeling for Interpretation of Infrared Images: U.S.G.S. Rept. U.S.G.S.-6D-71-D23.

Watson, K., 1973, Periodic Heating of a Layer over a Semi-Infinite Solid: Journal of Geophysical Research, V. 78, No. 26, pp. 5904-5910.

Watson, K., 1975, Geologic Applications of Thermal Infrared Images: Proc. I.E.E.E., 63, 128-136.

Watson, K., Rowan, L., and Offield, T., 1971, Application of Thermal Modeling in the Geologic Interpretation of Images: Proc. 7th Internat'l Symposium on Remote Sensing of Environment, Univ. Michigan, V. 3, pp. 2017-2041.

SCALE 1:62500

CONTOUR INTERVAL 24.4 METERS (80 FEET)
DOTTED LINES REPRESENT 6.1-METER (20-FOOT) CONTOURS
DATUM IS MEAN SEA LEVELS
ENGLISH UNITS WERE USED FOR THE PRINCIPLE MEASUREMENTS AND CALCULATIONS IN THIS FIGURE
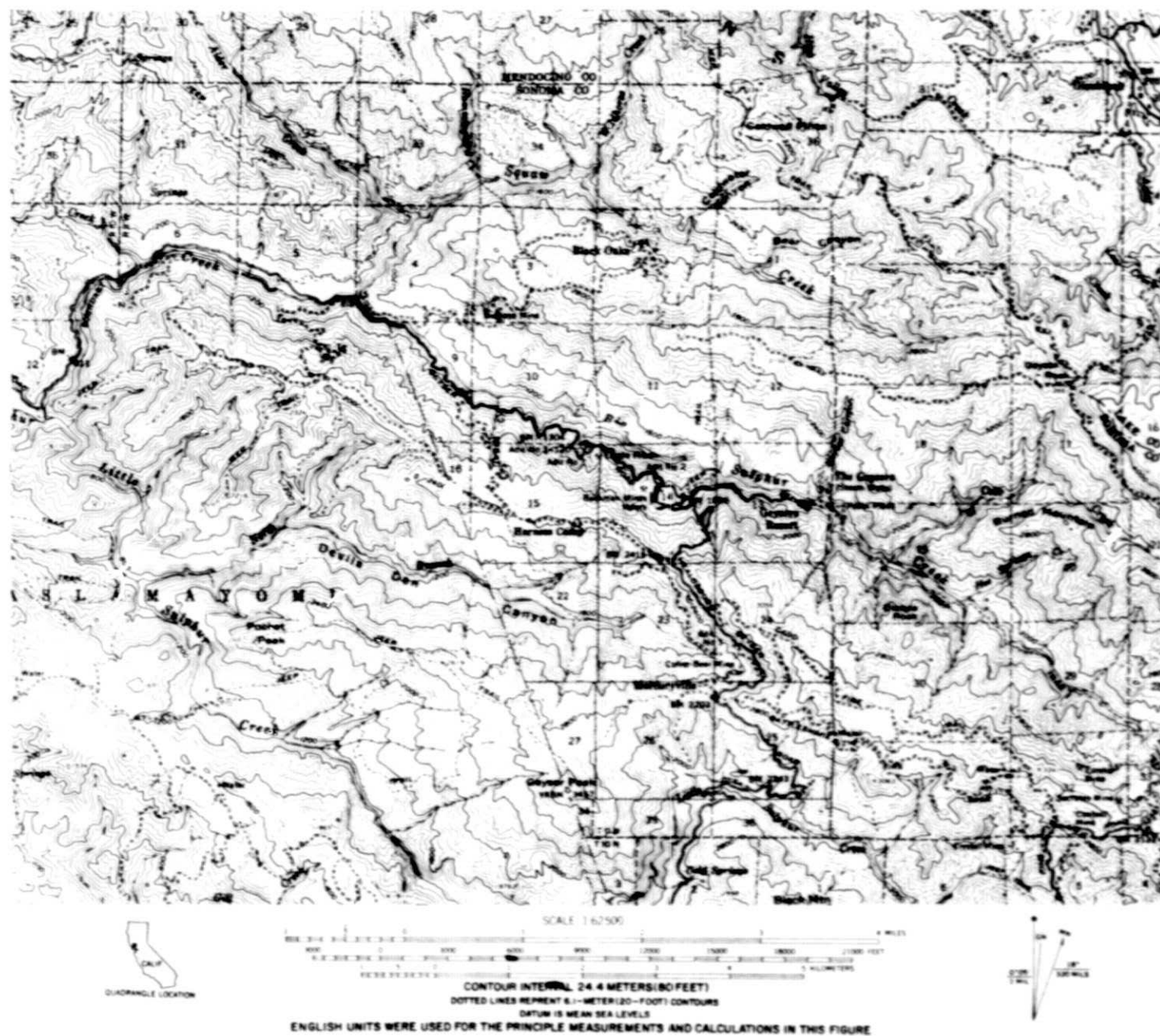
Fig. 1.   Topographic map of a portion of the Kelseyville 15' Quadrangle showing The
Geysers geothermal region

MAP EXPLANATION

STRATIGRAPHY

- ALLUVIUM (QUATERNARY)
- LANDSLIDE DEPOSITS (QUATERNARY)
- SERPENTINE (JURASSIC ?)
- METAMORPHOSED ULTRAMAFIC ROCKS (JURASSIC ?)
- SEDIMENTARY AND TECTONIC MÉLANGE (JURASSIC-CRETACEOUS)
- SEDIMENTARY BRECCIA (JURASSIC-CRETACEOUS)
- GRAYWACKE AND SHALE (JURASSIC-CRETACEOUS)
- GREENSTONE (JURASSIC-CRETACEOUS)
- CHERT (JURASSIC-CRETACEOUS)
- HYDROTHERMALLY ALTERED ROCKS

FRANCISCAN ASSEMBLAGE

MAP SYMBOLS

- CONTACT
- FAULT, DASHED WHERE APPROXIMATE, DOTTED WHERE CONCEALED, QUERIED WHERE UNCERTAIN; BALL ON DOWNTHROWN SIDE
- THRUST FAULT, DASHED WHERE APPROXIMATE, DOTTED WHERE CONCEALED; BARBS ON UPPER PLATE
- STREAM

SIMPLIFIED GEOLOGIC MAP OF THE GEYSERS AREA, SONOMA COUNTY, CALIFORNIA
(GEOLOGY AFTER Robert J. McLaughlin (1974)

Fig. 2.   Generalized geologic map of The Geysers area after McLaughlin (1974)
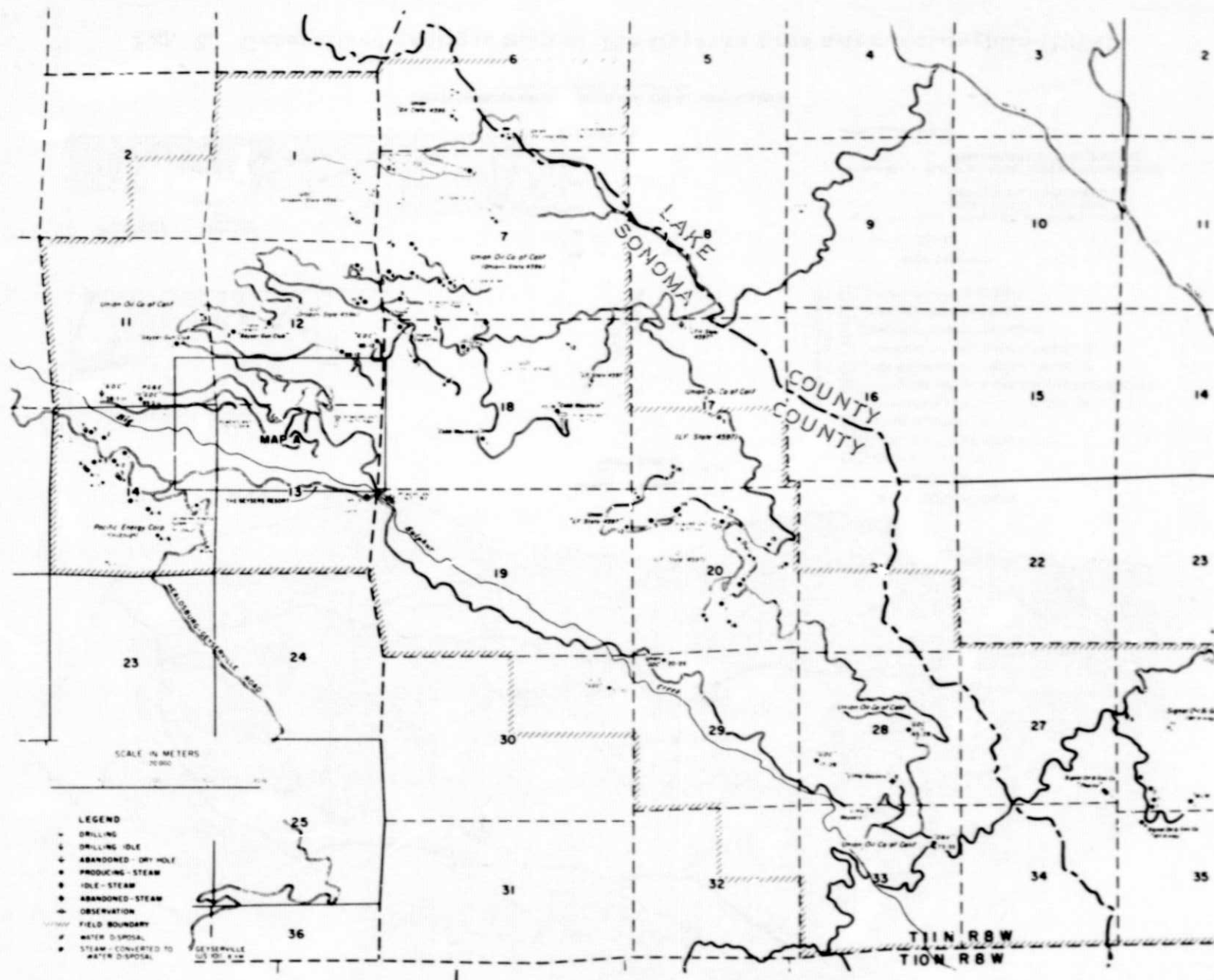
Fig. 3. Location map of geothermal wells and power plants in The Geysers area (after State of California Division of Oil and Gas, 1974)

LEGEND
- ⊸ DRILLING
- ⟡ DRILLING IDLE
- ⬥ ABANDONED - DRY HOLE
- ● PRODUCING - STEAM
- ◆ IDLE - STEAM
- ◆ ABANDONED - STEAM
- ⊶ OBSERVATION
- ////// FIELD BOUNDARY
- ⌀ WATER DISPOSAL
- ⌀ STEAM CONVERTED TO WATER DISPOSAL

LEGEND

SB - "Sulphur Bank"
HJ - "Happy Jack"
GDC - "Geysers Development Co"

MAP A
SCALE IN METERS
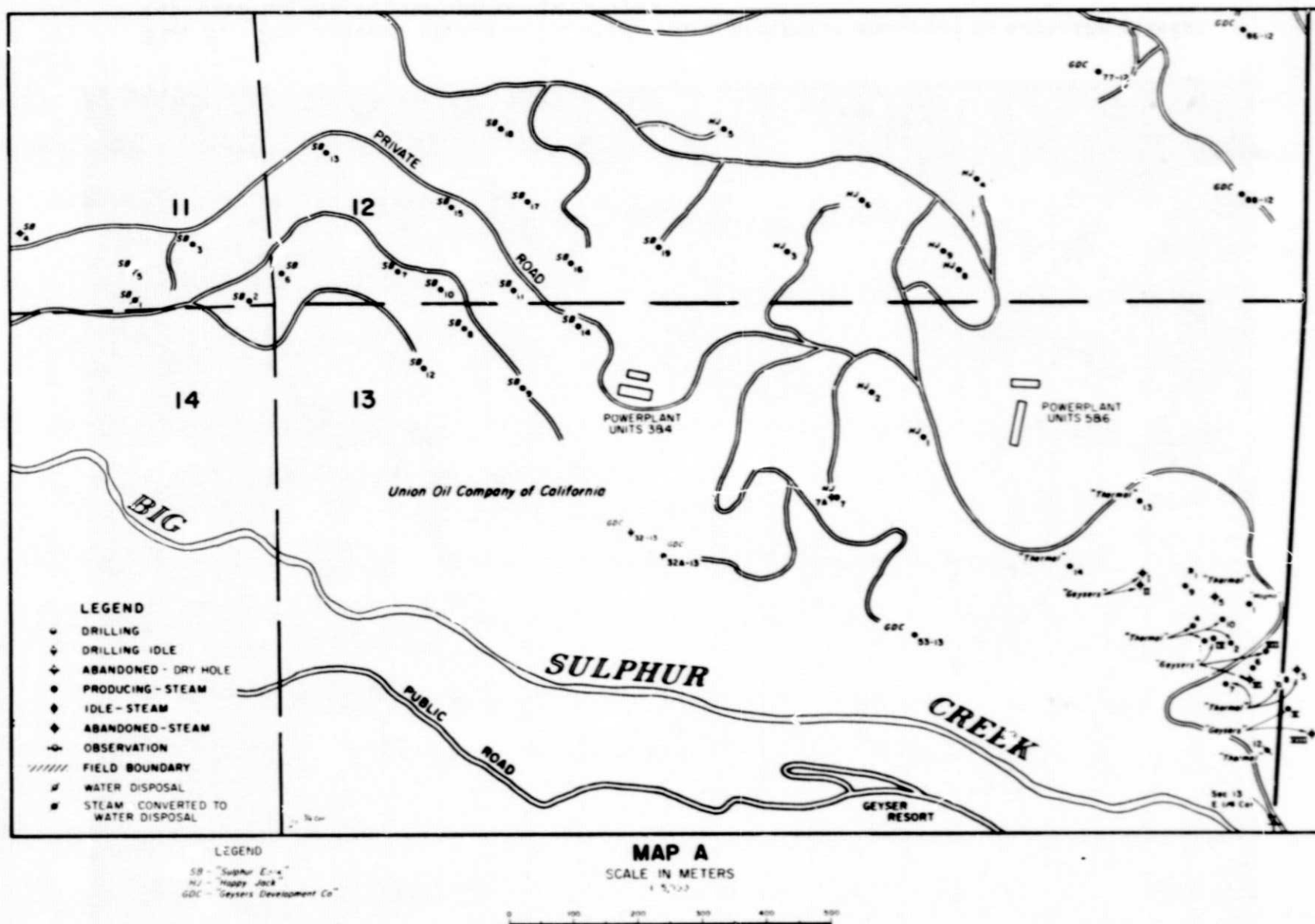
Fig. 4. Detailed map of The Geysers and adjacent areas showing locations of wells
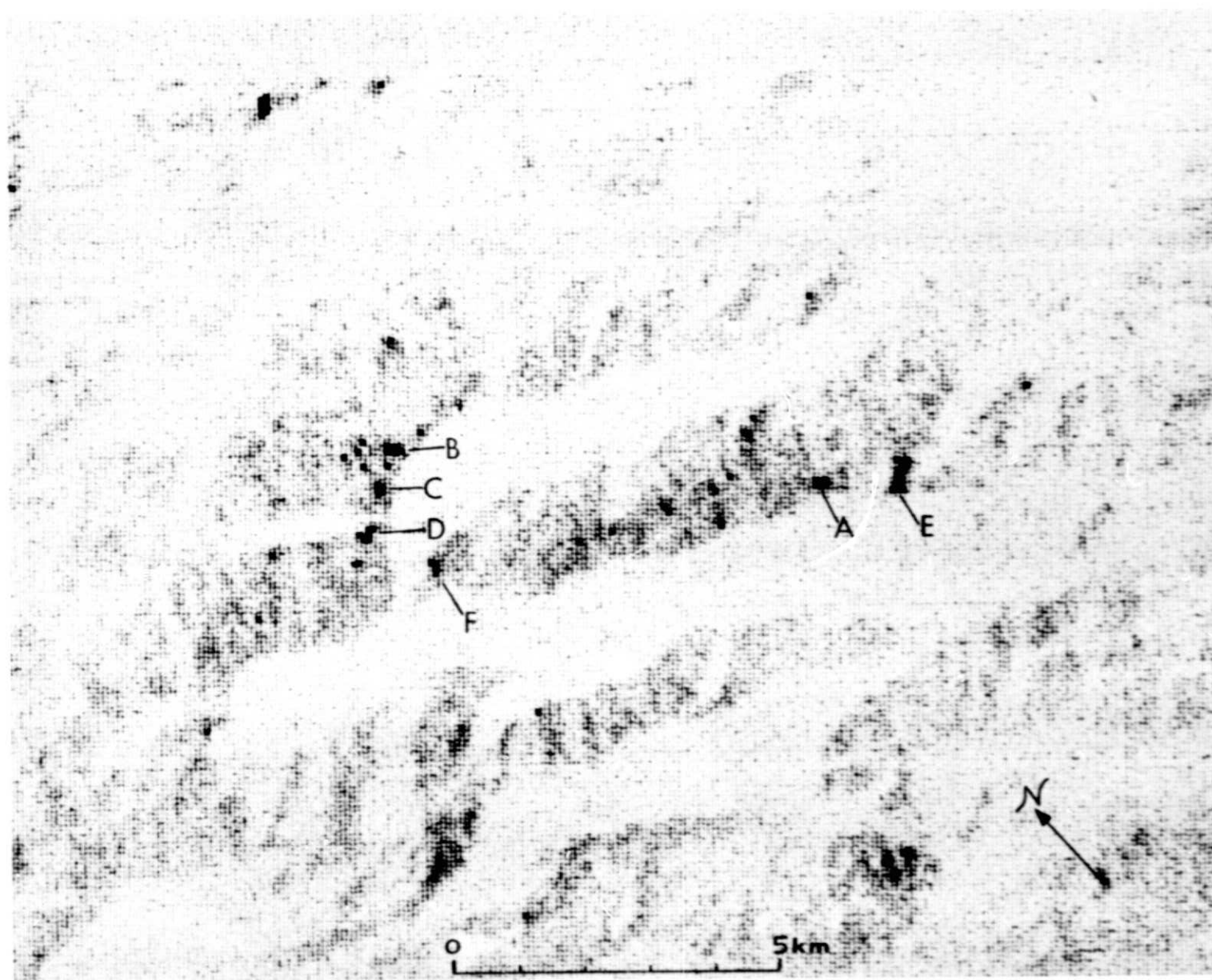
Fig. 5.   The Geysers region at 10. 2—12. 5 μm, computer enhanced to show the pixels
representing the 100 hottest temperatures
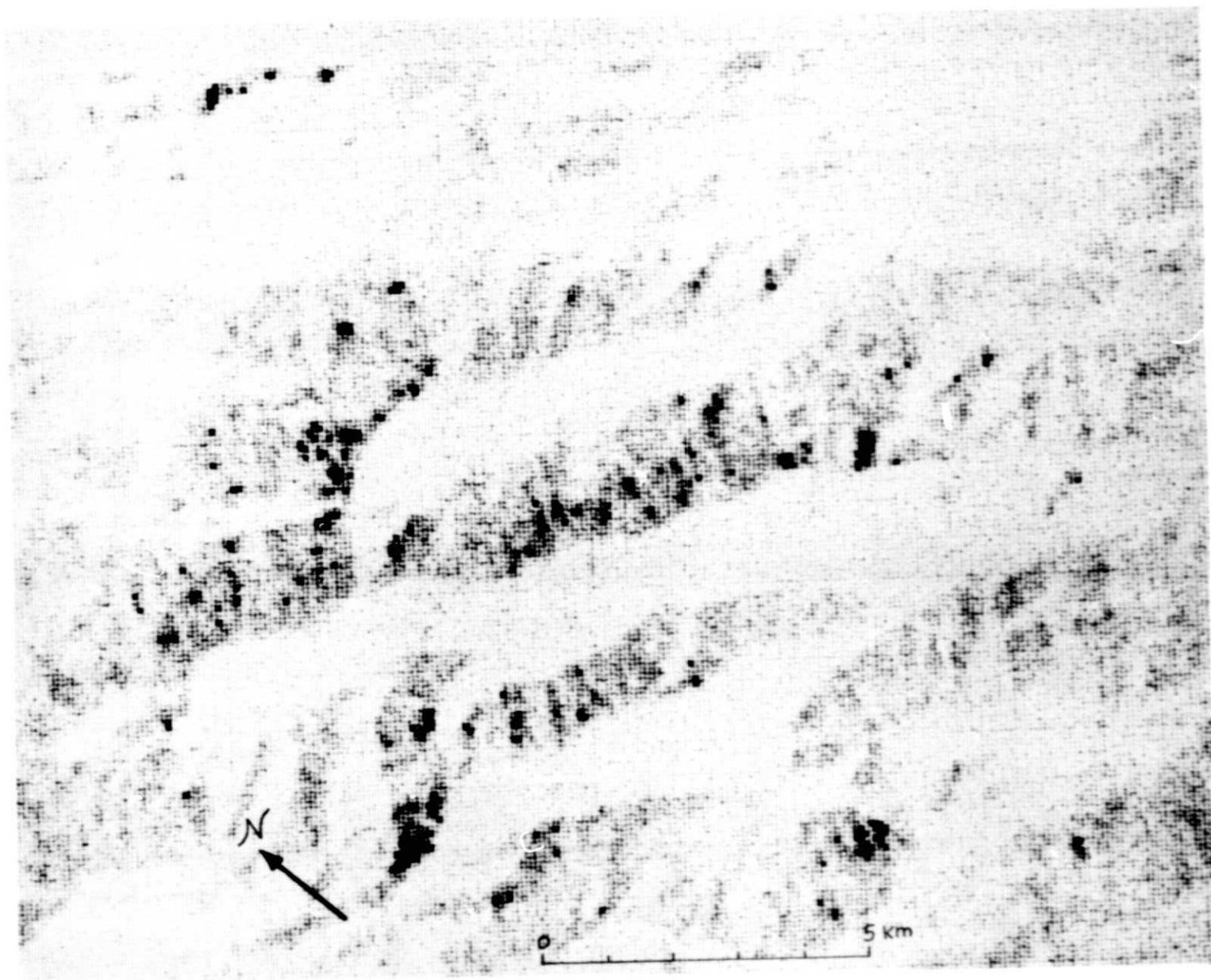
Fig. 6. The Geysers region at 10. 2—12. 5 μm, computer enchanced to show the pixels
representing the 300 hottest temperatures
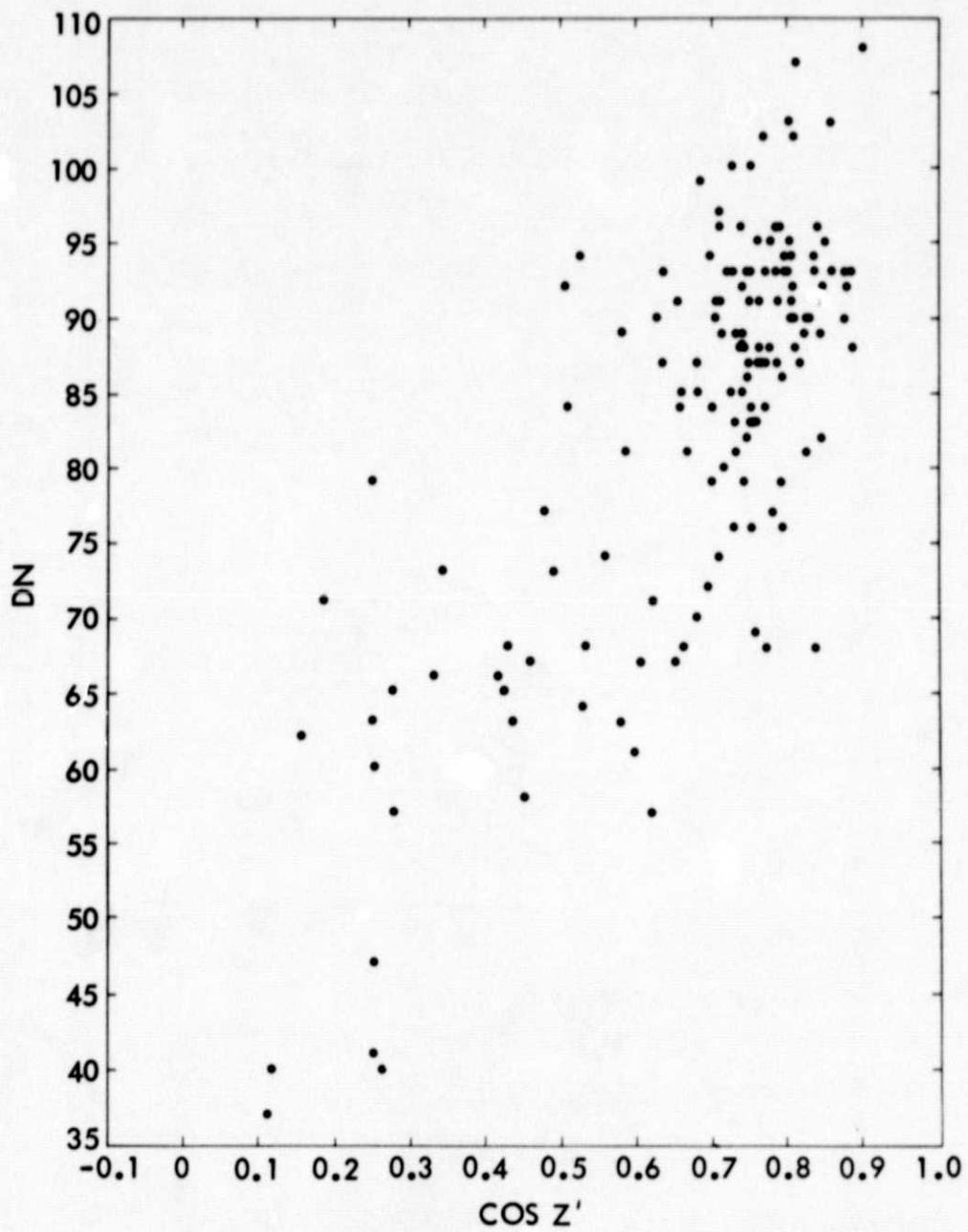
Fig. 7. Graph of DN versus cosine of the angle between slope normal and sun (Z')
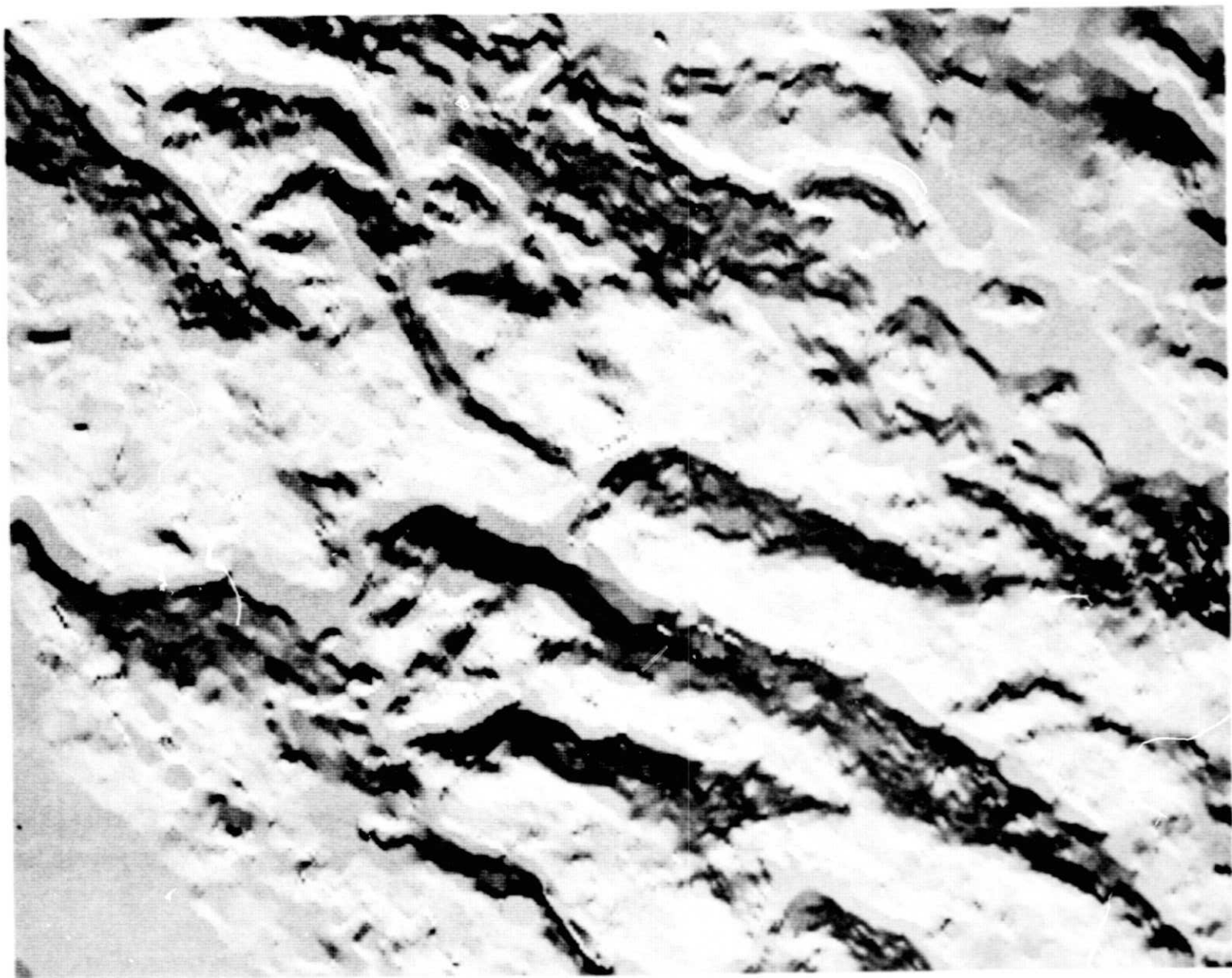
Fig. 8.   Computer simulated Skylab picture using digital topographic information and simulated solar radiation

Fig. 9.   Ratio picture of SDO 3 (. 56 to . 61 μm) to SDO 7 (. 68 to
. 78 μm)
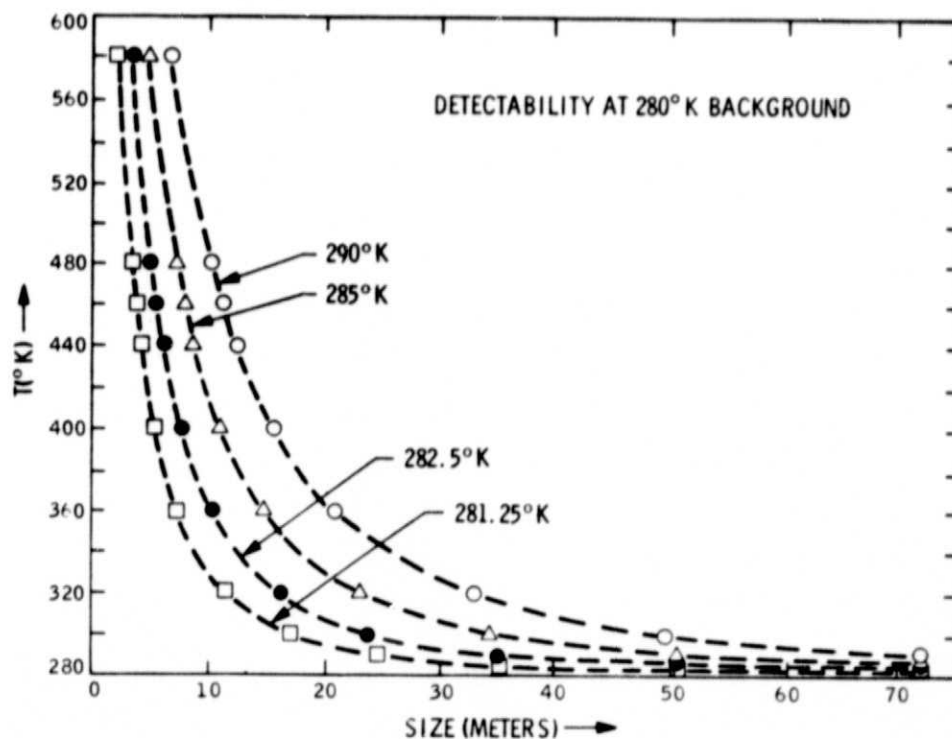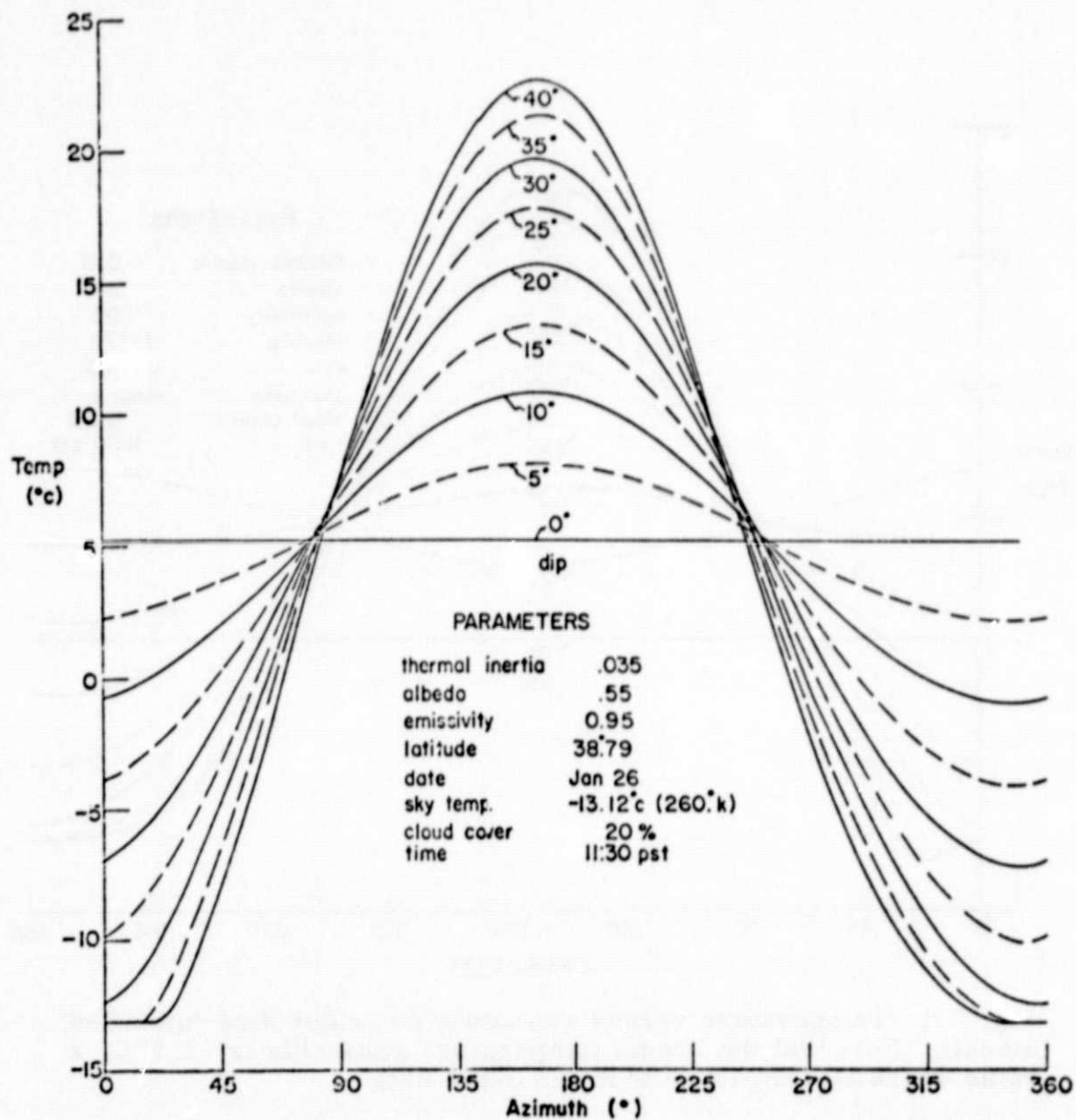

Fig. 10.   Detectability of thermal anomalies as a function of
size and temperature

Fig. 11. Temperature versus azimuth for various dips (initial model).
Note that the lowest temperature attainable is -13°C, a value which is
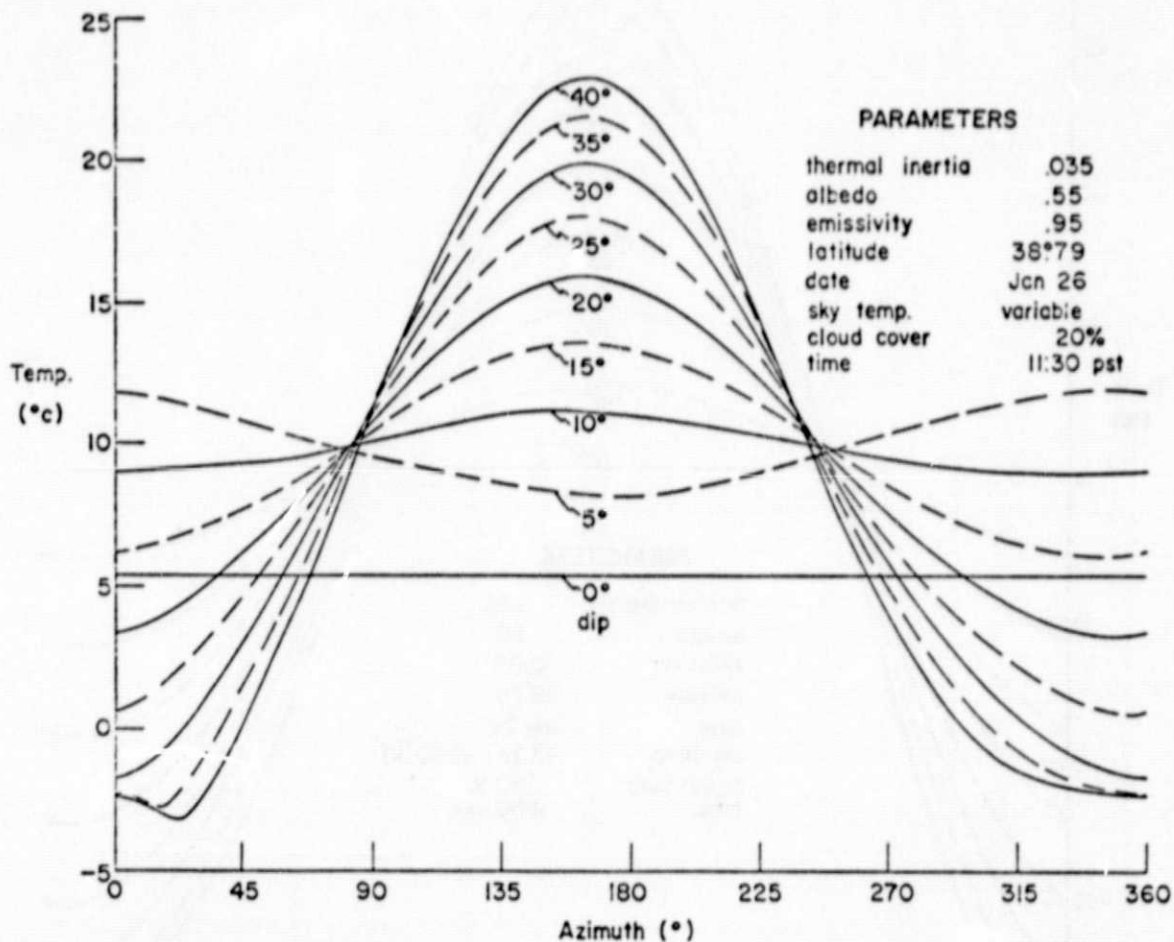considerably colder than the lowest temperature measured from the
S-192 data

Fig. 12. Temperature versus azimuth for various dips (modified model). Note that the lowest temperature attainable is -2.5°C, a value which is compatible with the S-192 data
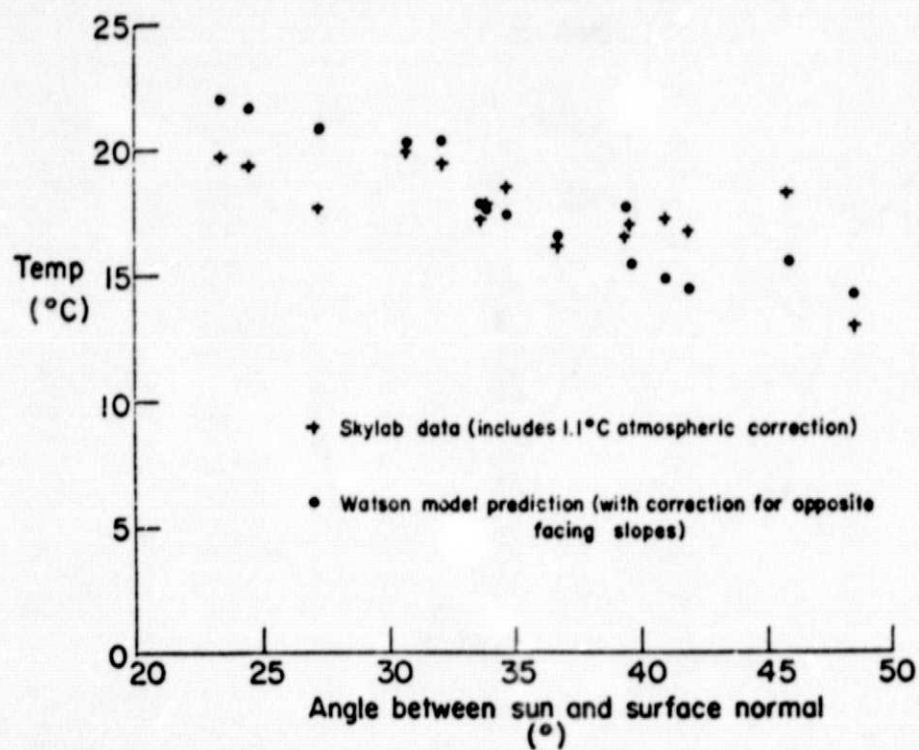
Fig. 13.   Temperature versus angle between the sun and surface normal for the 15 slopes used in the model
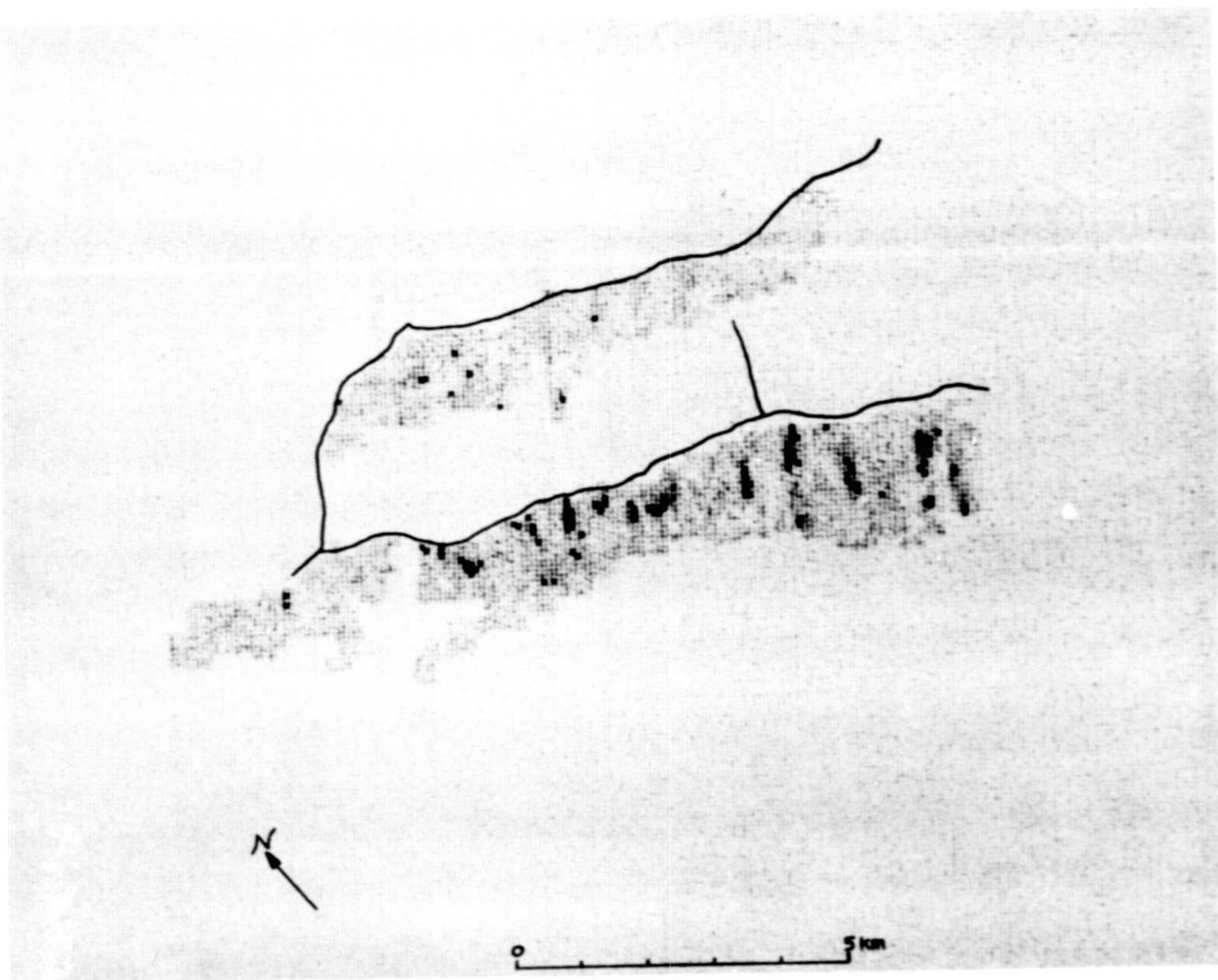
Fig. 14.   Extracted north-facing slopes of The Geysers region.   The 100 hottest ground areas are black